J Biol Inorg Chem (2015) 20:1253–1261
DOI 10.1007/s00775-015-1304-0

ORIGINAL PAPER

Histidine residues are important for preserving the structure and heme binding to the *C. elegans* HRG-3 heme-trafficking protein

Ortal Marciano[1] · Yoni Moskovitz[1] · Iqbal Hamza[2,3] · Sharon Ruthstein[1]

Received: 28 April 2015 / Accepted: 18 October 2015 / Published online: 3 November 2015
© SBIC 2015

Abstract *C. elegans* is a heme auxotroph that requires environmental heme for sustenance. As such, worms utilize HRG-3, a small heme-trafficking protein, to traffic heme from the intestine to extra-intestinal tissues and embryos. However, how HRG-3 binds and delivers heme remains unknown. In this study, we utilized electron paramagnetic resonance spectroscopy together with site-directed spin labeling, absorption spectroscopy, circular dichroism, and mutagenesis to gain structural and molecular insights into HRG-3. We showed that HRG-3 is a dimer, whereas H9 and H10 are significant residues that preserve a specific conformational state in the HRG-3 dimer. In the absence of H9 and H10, HRG-3 can still bind heme, although with a different affinity. Furthermore, the heme-binding site is closer to the N-termini than to the C-termini. Taken together, our results lay the groundwork for future mechanistic and structural studies of HRG-3 and inter-tissue heme trafficking in metazoans.

Keywords HRG-3 · Heme transfer · EPR · Site-directed spin labeling · Absorption spectroscopy

Abbreviations

CD	Circular dichroism
CW	Continuous wave
EPR	Electron paramagnetic resonance
MTSSL	1-Oxyl-2,2,5,5-tetramethyl-2,5-pyrroline-3-methyl) methanesulfonothioate
SDSL	Site-directed spin labeling

✉ Sharon Ruthstein
sharon.ruthstein@biu.ac.il

[1] Department of Chemistry, Faculty of Exact Sciences, Bar Ilan University, 5290002 Ramat-Gan, Israel

[2] Department of Animal and Avian Sciences, University of Maryland, College Park, MD 20742, USA

[3] Department of Cell Biology and Molecular Genetics, University of Maryland, College Park, MD 20742, USA

Introduction

Heme is an iron-coordinated tetrapyrrole that serves as an electron carrier and a catalyst for redox reactions [1, 2]. In addition, it is a hydrophobic cytotoxic molecule unlikely to freely diffuse within a cell. Hence, specific molecules and pathways must exist to facilitate heme delivery to distinct intra- and inter-cellular destinations [3–5]. Although significant strides have been made towards better understanding the mechanism underlying the regulation of heme synthesis and its degradation in eukaryotes, little is known about the heme transfer mechanism in eukaryotes. Studies of heme transporters in bacteria have provided a molecular understanding of protein function, but these transporters do not have close homologs in animals [3, 6].

Caenorhabditis elegans (*c. elegans*) is a heme auxotroph and thus relies solely on environmental heme for growth and reproduction [7–11]. Since organismal heme levels can be externally manipulated in a controlled manner, *C. elegans* serves as an ideal genetic animal model for studying the molecular basis of heme trafficking. Worms acquire environmental heme by importing heme into the intestine through the coordinated actions of HRG-1 and HRG-4 membrane-bound heme transporters. Heme from the intestine is mobilized by HRG-3, a secreted protein that exports maternal heme to extraintestinal tissues [3–5]. HRG-3 binds heme at a stoichiometry of two monomers to one heme molecule. Although deletion of HRG-3 had no appreciable effect on adult worms grown in low levels of

heme, their progeny were either unable to hatch or growth was arrested at the first larval stage. Even though a functional homolog of HRG-3 in mammals has yet to be discovered, it is reasonable to speculate that during development, a heme-delivery protein or chaperone may facilitate the targeted delivery and redistribution of heme between certain tissues and cell types [6, 8]. HRG-3 is a 71-amino acid protein with an N-terminal hydrophobic segment of 29 amino acid residues that target HRG-3 to the secretory pathway. The hydrophobic signal peptide is cleaved in the mature protein, resulting in a small, soluble protein that is secreted from the intestine. By binding and delivering heme to developing embryos, this protein performs the function of a hemochaperone. In vitro expression revealed that the mature HRG-3 binds heme in both the ferrous (Fe(II)) and the ferric (Fe(III)) oxidation states [8]. Although proteins may contain heme-binding motifs such as CXXCH or CXXC, there are examples, such as bacterial hemochaperone CcmE, in which a single residue in the right environment is sufficient to bind heme [3, 12]. This makes the study of heme-binding proteins and heme coordination environments more challenging, based solely on linear protein sequences. Indeed, HRG-3 lacks cysteine residues but contains two histidine residues.

In the current study, we utilized continuous-wave electron paramagnetic resonance (CW-EPR) spectroscopy together with site-directed spin labeling (SDSL), absorption spectroscopy, circular dichroism (CD), and mutagenesis to explore heme binding to HRG-3. Gaining a structural and molecular understanding of HRG-3 will assist in elucidating its X-ray crystal structure and will shed light on the mechanisms underlying heme transfer mediated by hemochaperones.

Materials and methods

HRG-3 expression and purification

The expression of HRG-3 was achieved using the expression vector sequences pYTB12 (5′ primer-GTTGTACAGAATGCTGGTCATATGGAACCGCCTGCAGAAAAAACG and 3′ primer- GTCACCCGGGCTCGAGGAATTTTCTGAGTCGG GTCAATGCG). This amplicon was cloned to the pYTB12 vector by the free ligation PCR technique [13]. This construct encodes for a fusion protein composed of HRG-3, Intein, and chitin-binding domains; it was transformed into the *E. coli* strain BL21 (DE3). The HRG-3 construct was expressed in BL21 cells, which were grown to an optical density of 0.6–0.8 at 600 nm and induced with 1 mM isopropyl-*β*-D-thiogalactopyranoside (CALBIOCHEM) for 18 h at 18 °C. The cells were then harvested by centrifugation at 10,000×*g* for 30 min, after which the pellets were subjected to three freeze–thaw cycles. Pellets were resuspended in lysis buffer (25 mM NaH_2PO4, 150 mM NaCl, pH 8.8) and sonicated by six bursts of 1 min, each with a 1-min cooling period between each burst (65 % amplitude). After sonication, the cells were centrifuged and the soluble fraction of the lysate was passed through a chitin bead column (New England Biolabs), allowing the HRG-3 fusion to bind to the resin via its chitin-binding domain. The resin was then washed with 50 column volumes of lysis buffer. To induce the intein-mediated cleavage, the beads were incubated in 50 mM dithiothreitol (DTT), 0.25 % *n*-dodecyl-*β*-D-maltoside (DDM), 25 mM NaH_2PO4, and 2 M NaCl, pH 8.8 for 40 h at room temperature. HRG-3 was then eluted and analyzed by SDS-PAGE (Tricine 19 %) and mass spectroscopy. The protein's mass was confirmed by MALDI–TOF MS–Autoflex III–TOF/TOF mass spectrometer (Bruker, Bermen, Germany) equipped with a 337-nm nitrogen laser.

Mutations were carried out using the free ligation PCR technique [13]. Table 1 lists all the mutations studied in this research.

A mega-primer was created in the following manner: HRG-3_#1 using HRG-primers 1&2, HRG-3_#2 mutant using HRG-primers 3&2, HRG-3_#3 mutant using HRG-primers 4&2, HRG-3_#4 mutant using HRG-primers 5&2, HRG-3_#5 mutant using HRG-primers 1&6, HRG-3_#6 mutant using HRG-primers 3&6, HRG-3_#7 mutant using HRG-primers 4&6, HRG-3_#8 mutant using HRG-primers 5&6, and HRG-3_#9 mutant using HRG-primers 7&2. These mega-primers were used for another PCR in which the pYTB12 vector was used as template.

Primer list: HRG1 + :GTTGTACAGAATGCTGGTCATATGAAAAGTGGATATTCTAAGAAT; HRG2 − :GTCACCCGGGCTCGAGGAATTTTATCCACCAAAAAACGAGTCACTCG; HRG3 + :GGATATTCTAAGAATGCTCATCTTTTCC; HRG4 + :GGATATTCTAAGAATCATGCTCTTTTCC; HRG5 + :GGATATTCTAAGAATGCTGCTCTTTTCC; HRG6 − :GTCACCCGGGCTCGAGGAATTTTAACATCCACCAAAAAACGAGTCACTCG; HRG7 + :GTTGTACAGAATGCTGGTCATATGTGTAAAAGTGGATATTCTAAGAA;

Heme incorporation into HRG-3 solution

15 µL of hemin (20 mM) (Frontier Scientific) dissolved in dimethyl sulfoxide (DMSO, Bio lab) were added to a 750 µL HRG-3 solution. The mixture was vortexed for 1 h (10 °C), followed by sonication (10 min). To remove excess hemin, lysis buffer was added to the solution, up to a volume of 2 mL, and the mixture was centrifuged

Table 1 HRG-3 mutants studied in this research

#	HRG-3 mutant's sequence
1	MKSGYSKNHHLFRPKNLQTDSEEGFWNNVYFVITASDSFFGG (WT HRG-3)
2	MKSGYSKNAHLFRPKNLQTDSEEGFWNNVYFVITASDSFFGG
3	MKSGYSKNHALFRPKNLQTDSEEGFWNNVYFVITASDSFFGG
4	MKSGYSKNAALFRPKNLQTDSEEGFWNNVYFVITASDSFFGG
5	MKSGYSKNHHLFRPKNLQTDSEEGFWNNVYFVITASDSFFGGC-R1[a] (cR1 HRG-3)
6	MKSGYSKNAHLFRPKNLQTDSEEGFWNNVYFVITASDSFFGGC-R1
7	MKSGYSKNHALFRPKNLQTDSEEGFWNNVYFVITASDSFFGGC-R1
8	MKSGYSKNAALFRPKNLQTDSEEGFWNNVYFVITASDSFFGGC-R1
9	R1-NMKSGYSKNHHLFRPKNLQTDSEEGFWNNVYFVITASDSFFGG (nR1 HRG-3)

[a] R1 represents the *S*-(2,2,5,5-tetramethyl-2,5-dihydro-1H-pyrrol-3-yl)methyl methanesulfonothioate (MTSSL) spin label attached to the cysteine residue

in a concentration tube (Microsep Advance Centrifugal Devices, 2 kDa cutoff). When 750 µL was reached, the upper 500 µL were transferred to a second centrifugation step. This procedure was repeated three times. The final protein solution was concentrated to a final volume of 0.1 mM protein.

HRG-3 spin labeling

The protein was spin-labeled with *S*-(2,2,5,5-tetramethyl-2,5-dihydro-1*H*-pyrrol-3-methyl) methanethiosulfonothiate (MTSSL, TRC) at the targeted cysteine. HRG-3 was initially incubated with 10 mM DTT for 4 h. DTT was removed by Microsep Advance Centrifugal Devices (2 kDa cutoff) against lysis buffer three times at 3220×*g* at 8 °C for 20 min. MTSSL (MW 264.3 g/mol) was added to the HRG-3 solution at a ratio of 1:50 = [HRG-3]:[spin label], a 50-fold molar excess of MTSSL, and then mixed overnight at 4 °C in the dark. The free spin label was removed by the microsep advance centrifugal devices against a lysis buffer eight times at 3220×*g* at 8 °C for 20 min. This procedure ensures that no free spin label was left, and that only the selected cysteine residues are labeled. The mass of the spin-labeled protein was confirmed by a mass spectrometer. The final protein solution was concentrated to a final volume of 0.1 mM protein [14].

Glutaraldehyde crosslinking

Treatment with glutaraldehyde was conducted by mixing 50 µg (20 µL) of interacting protein in a 20 mM (70 µL) sodium phosphate and a 0.15 M NaCl solution at pH 8 (PBS 10 ×), which was then reacted with 10 µL of glutaraldehyde solution, incubated, and finally shaken for 10 min at 37 °C. The reaction was terminated by the addition of 10 µL of 1 M Tris–HCl at pH 8.

CW-EPR

Spectra were recorded using an E500 Elexsys Bruker spectrometer operating at 9.0–9.5 GHz. The spectra were recorded at room temperature (RT) at microwave power of 20.0 mW, modulation amplitude of 1.0 G, a time constant of 60 ms, and a receiver gain of 60.0 dB. The samples were measured in 0.8-mm capillary quartz tubes (vitrocom). The solutions that were measured at low temperature were then mixed with 20 % glycerol, and were measured in a 3.0-mm Wilmad quartz tube.

Absorption spectra

UV–Vis measurements were carried out on a Varian Cary 5000 spectrophotometer at RT, using a 1.0-cm quartz cuvette.

CD

Protein solutions were dialyzed for 4 h to remove salts against water in a Midi Geba-flex tube, with 1 kDa cutoff before measurements. CD measurements were carried out using a Chirascan spectrometer (Applied Photophysics, UK). The measurements were performed at RT in a 1.0-cm quartz cuvette, and the spectra were recorded from 260 to 190 nm with a step size and a bandwidth of 0.5 nm. The CD signal was averaged for 10 s every 2 nm for 10 scans.

The dissociation constant analysis

The dissociation constant, K_d, of heme to HRG-3 was calculated as follows. The chemical reaction is

$$x[\text{heme}] + [\text{HRG-3}] \rightarrow [\text{heme - HRG - 3}]$$

where x is the number of heme molecules bound per HRG-3 monomer.

$$K_d = \frac{[\text{heme}]_{eq}^{x}[\text{HRG-3}]_{eq}}{[\text{heme-}HRG-3]_{eq}}.$$

$$[\text{heme}]_{eq} = [\text{heme}] - [\text{heme}]_{bound}.$$

$$[\text{HRG-3}]_{eq} = [\text{HRG-3}]_0 - [\text{HRG-3}]_{reacted}.$$

$$[\text{heme - HRG-3}] = [\text{HRG-3}]_{reacted}.$$

$$[\text{HRG-3}]_{reacted} = \frac{1}{x}[\text{heme}]_{bound}.$$

$$n = \frac{[\text{heme}]}{[\text{HRG-3}]_0}.$$

$$K_d = \frac{[n[\text{HRG-3}]_0 - [\text{heme}]_{bound}]^x \left[[\text{HRG-3}]_0 - \frac{1}{x}[\text{heme}]_{bound}\right]}{\frac{1}{x}[\text{heme}]_{bound}}.$$

$$\text{Absorption} \approx [\text{heme}]_{bound}.$$

In our experiments, n is the equivalent of [heme] added and $[\text{HRG-3}]_0 = 0.1$ mM. The K_d values were calculated for various parameters of x between 0.5 and 2.0.

Results and discussions

In this study, we aimed to gain structural information about the ferric heme-binding site of HRG-3, one of the few heme chaperones identified thus far in eukaryotes. Purified HRG-3 exhibits solubility characteristics and gradually precipitates at neutral pH. Therefore, protein concentrations as low as 0.1 mM were used for all measurements. Initially, we expressed the mature WT HRG-3 protein. Figure 1 shows purified WT HRG-3 confirmed by SDS-PAGE (Fig. 1a) and MALDI mass spectrometry (Fig. 1b). Despite that HRG-3 lacks cysteine residues, it has two conserved histidine residues at positions 9 and 10, which may participate in heme coordination. To determine the effect of His residues on heme binding, we prepared several mutants, which are listed in Table 1.

The HRG-3 protein and its mutants were analyzed by low-temperature (120 K) CW-EPR spectroscopy. To ensure that isolated hemin in the solution does not contribute to the EPR signal, several sonication and centrifugation steps were taken to remove unbound hemin from the solution. Figure 2a presents the EPR spectra of 0.2 mM hemin in buffer after various steps of sample preparation. The broad signals at $g = 5.7$ and $g = 4.2$, which appear after mixing hemin in buffer, indicate the presence of hemin aggregates in the solution. These signals gradually disappear after centrifugation is performed to remove free hemin. After removal of free hemin, we measured the EPR spectra of various HRG-3 mutants. Figure 2b presents the CW-EPR spectra of ferric heme bound to WT HRG-3 (#1 in Table 1), H9A mutant (#2), H10A mutant (#3), and H9A/H10A double mutant (#4). For a comparison, the signal of an empty capillary is also presented. Although the signal

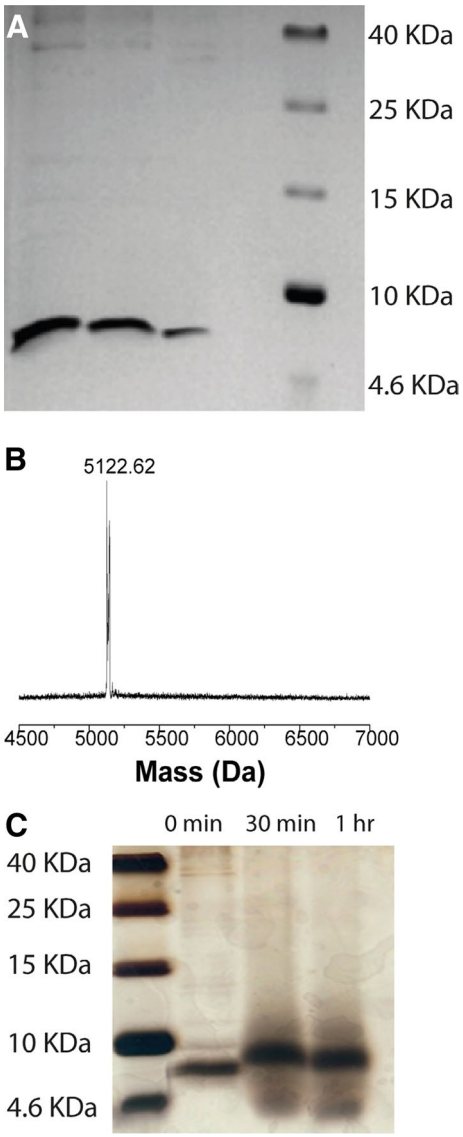

Fig. 1 **a** SDS-PAGE gel picture of purified HRG-3. **b** MALDI mass spectrometry of WT HRG-3. **c** SDS-PAGE gel picture of HRG-3 dimer, before and after crosslinking with glutaraldehyde

was very low, possibly due to the low protein concentration (0.1 mM) in the solution, a clear signal around $g \approx 4.2$ was observed for all mutants. This signal was proposed to arise from the ± 3/2 Kramers doublet of a $S = 5/2$ ground spin multiplet, suggesting the existence of a ferric heme in a rhombic coordination in relation to the protein [15, 16]. Mutations of H9A and double mutation of H9A/H10A slightly increased the line width of the $g \approx 4.2$ signal, which might be due to some distortion in the heme environment. The fact that all mutants exhibited a $g \approx 4.2$ signal in the EPR spectrum indicates that single and double histidine mutants are capable of binding heme.

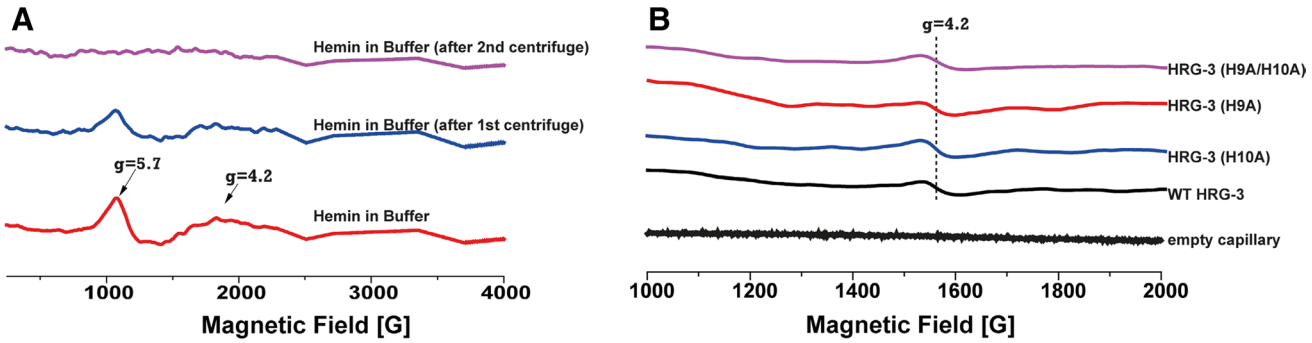

Fig. 2 **a** CW EPR spectra at 120 K for 0.2 mM hemin in buffer solution at various centrifugation cycles. **b** CW EPR spectra at 120 K for various HRG-3 mutants in the presence of hemin

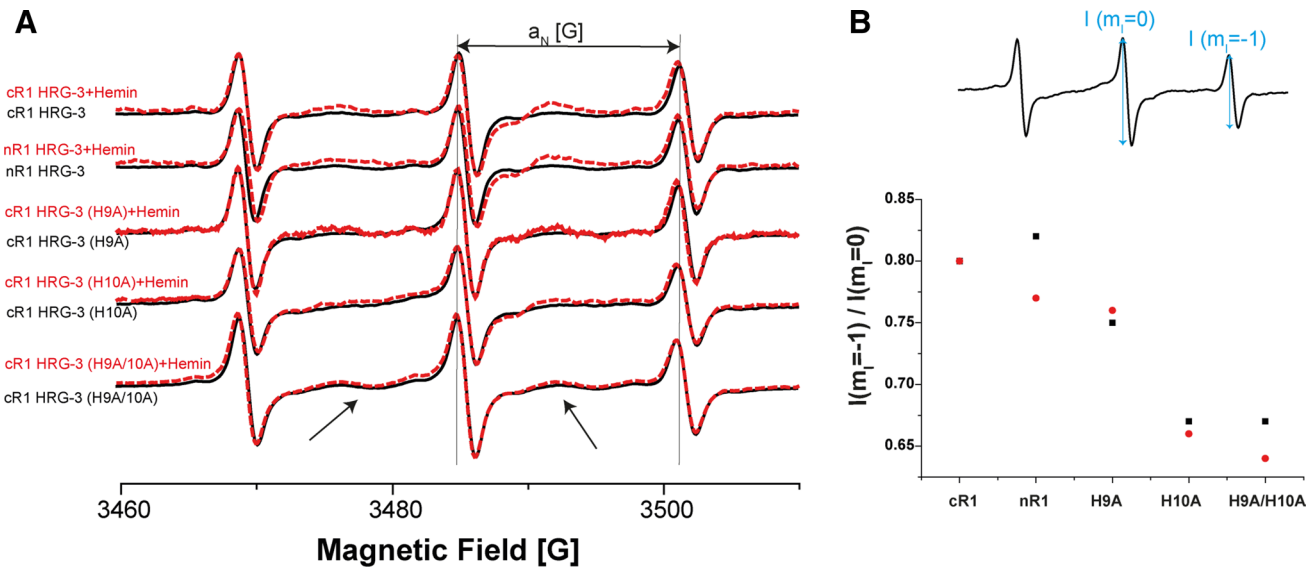

Fig. 3 **a** CW-EPR spectra of spin-labeled HRG-3 mutants conducted at RT (*black solid lines*), and in the presence of hemin (*red dashed lines*). The *arrows* highlight the characteristic signals for dipolar or exchange interactions between paramagnetic centers. **b** The $I(m_I = -1)/I(m_I = 0)$ value for various HRG-3 mutants in the presence (*red circles*) and absence (*black squares*) of hemin

To further explore changes in the conformational state of the protein upon its coordination to heme, we expressed HRG-3 with a cysteine residue inserted into its C-terminus (cR1 HRG-3, #5 in Table 1). The cysteine residue was labeled with a MTSSL spin label. The MTSSL is stable in solution and generally causes minimal perturbation to the protein and its function [17–19]. Since HRG-3 is a small protein, it is preferable to add cysteine residues only at the protein termini, to prevent distortion of the protein's structure. We expressed and purified HRG-3 labeled at the C-terminus with the following mutations: H9A (#6), H10A (#7), double mutations H9A/H10A (#8), and HRG-3 labeled on its N-terminus (nR1 HRG-3, #9). Next, we used RT CW-EPR spectroscopy since it is usually the most efficient way to record an EPR spectrum, typically providing the g-factor and reporting on interactions between a paramagnetic center and nearby nuclei (hyperfine interaction) [20]. Additionally, CW-EPR experiments performed at RT can provide information on the dynamics of a spin label in its local environment [21–27]. The RT CW-EPR spectra of the various spin-labeled mutants are presented in Fig. 3a in the absence (black solid lines) and presence of hemin (red solid lines). The spectra show several interesting characteristics. First, all line shapes are characterized by the fast dynamics of the nitroxide spin label, resulting in an isotropic nitroxide EPR spectrum, which indicates that the protein is relatively flexible, probably owing to its small size. Second, all spectra are characterized by dipolar or exchange interactions, highlighted by black arrows. The dipolar interaction is noticeable even without incorporating hemin into the protein solution. This suggests that two monomers of HRG-3 are in proximity to each other, and may form a

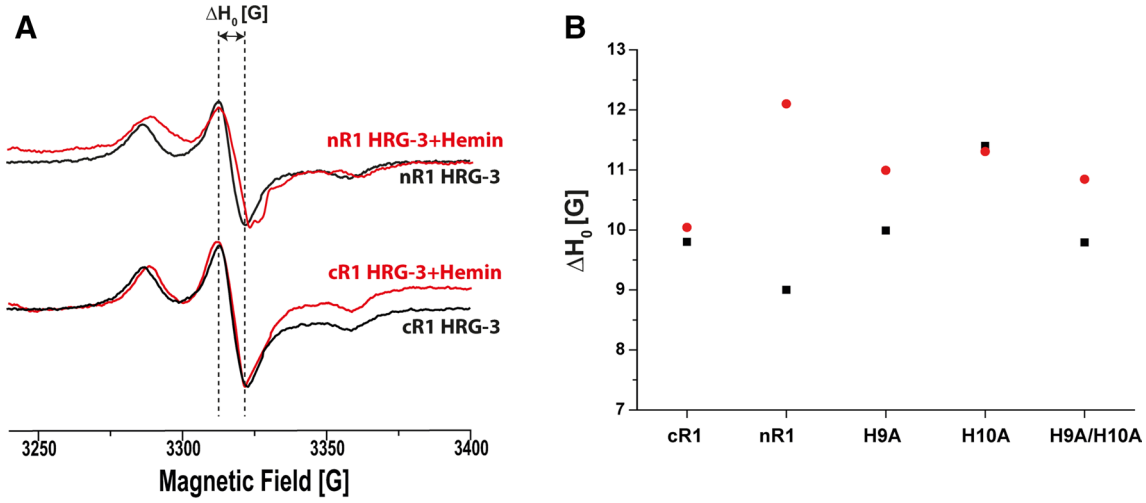

Fig. 4 **a** CW EPR spectra at 120 K for HRG-3 spin-labeled at its *C*-terminal and at its *N*-terminal, in the presence (*red line*) and absence (*black line*) of hemin. **b** The change in the central line width, ΔH_0, for the various spin-labeled HRG-3 mutants in the presence (*red circles*) and absence (*black squares*) of hemin

dimer. This is consistent with the data reported by Chen et al. [8], suggesting that each heme is coordinated by two HRG-3 monomers. Indeed, crosslinking experiments with glutaraldehyde for either 30 or 60 min showed a band on SDS-PAGE that appeared closer to 10 kDa, confirming HRG-3 dimerization through lysine residues (Fig. 1c). In addition, a decrease in the ratio between the intensity of the $m_I = -1$ resonance line and the $m_I = 0$ resonance line was observed for the H9A, H10A, and H9A/H10A mutations (Fig. 3b). A ratio of $I(m_I = -1)/I(m_I = 0) \cong 1$ characterizes fast dynamics, whereas a smaller ratio indicates the slower dynamics of the spin label attached to the protein. This result suggests that the spin label attached to the C-terminus of various mutants has slower dynamics as compared with WT HRG-3 (cR1 HRG-3), suggesting that the mutants have a different conformational state. In addition, a decrease of 0.2 ± 0.05 G in the hyperfine coupling (the a_N value) was observed for the H10A and H9A/H10A mutations, indicating that the spin label attached to the C-terminus in these mutants have a slightly more hydrophobic environment, thus confirming that the mutants have a different conformational state.

In the presence of hemin, an increase in the dipolar interaction, characterized by an increase in the line width, was observed for all mutants owing to the presence of a paramagnetic center. This indicates that heme can indeed bind mutant forms of HRG-3. A slightly larger increase in the line width was observed for nR1 HRG-3, suggesting that the heme-binding site is closer to the N-terminus of HRG-3. Nevertheless, for the H10A and H9A/H10 mutants, a smaller increase in the dipolar coupling was detected in the presence of hemin. This may suggest that not only is the affinity of hemin to these mutants lower, but the heme-binding environment in these mutants is different compared with WT HRG-3. Furthermore, the presence of heme affected the dynamics of the nR1 HRG-3 mutants more than HRG-3 mutants labeled at the C-terminus as discerned by a reduction in the $I(m_I = -1)/I(m_I = 0)$ ratio, suggesting that the heme-binding site should be closer to the N-terminus.

CW-EPR measurements were also conducted at 120 K using the spin-labeled HRG-3 mutants to compare the change in the line width of the rigid-limit spectra upon heme coordination for various mutants (Fig. 4). An increase in the line width at low temperature is correlated with an increase in the dipolar interaction between two paramagnetic centers. The low-temperature CW-EPR data show that the addition of hemin (the red squares in Fig. 4b) increased the line width of a spin label attached to the C-terminus of WT HRG-3 only slightly, whereas a striking increase in the line width was observed when the spin label was attached to the N-terminus of HRG-3. Clear changes in the line width were observed by CW-EPR when the distance between two paramagnetic centers is smaller than 2.0 nm. This result supports the concept that the binding site of heme is closer to the N-terminus of HRG-3 rather than the C-terminus. Moreover, for the H10A mutation, a larger line width was observed as compared with cR1 WT HRG-3 in the presence and absence of hemin. This suggests that the protein with this mutation has a different conformational state, where the two spin labels attached to the C-terminus are closer in H10A than in cR1 WT HRG-3. Furthermore, H9A and H9A/H10A exhibited a larger increase in the line width upon heme binding, compared with cR1 WT HRG-3, suggesting that the heme binding site is slightly different in the presence of these mutations. In summary, the RT and

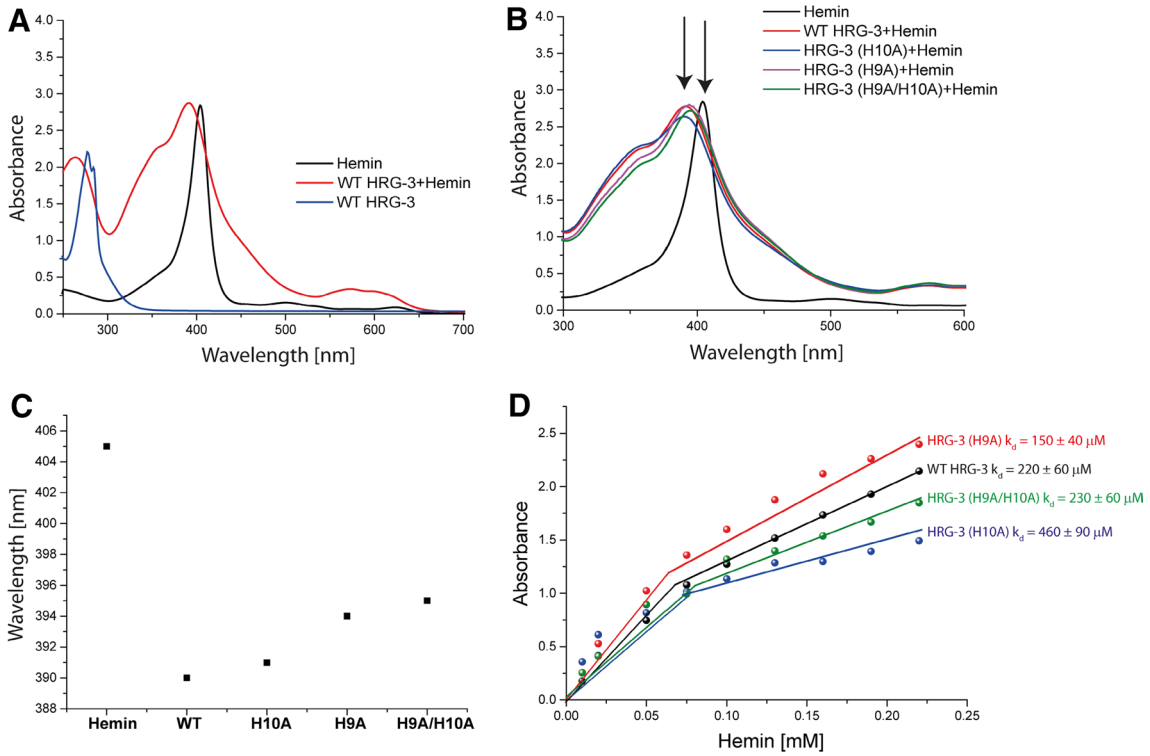

Fig. 5 **a** Absorption spectra of WT HRG-3 in the presence and absence of hemin, and for hemin solution. **b** Absorption spectra of various HRG-3 mutants in the presence of hemin, and for hemin solution. **c** The maximum absorption wavelength of various HRG-3 mutants in the presence of hemin. **d** The change in the absorption amplitude at 400 nm as a function of [Hemin] for various HRG-3 mutants

low-temperature CW EPR data suggest that H9 and H10 are important residues for preserving a specific conformational state of the protein as well as the heme-binding site.

We next determined the absorption spectra of HRG-3 in the presence and absence of hemin (Fig. 5a). The absorption spectra of WT HRG-3 are characterized by absorption around 280 nm, which results from the aromatic ring absorption (tryptophan or tyrosine residues). An absorption peak around 400 nm corresponds to the absorption spectra of hemin solution with a maximum at 405 nm. The spectrum of WT HRG-3 in the presence of hemin shows characteristic peaks between 300 and 650 nm, which is indicative of heme binding [8, 28]. The largest and broadest absorption occurred around a maximum of 390 nm. Although the H10A, H9A, and H9A/H10A HRG-3 mutants all exhibited absorption spectra similar to WT HRG-3 (Fig. 5b), a shift in the maximal absorbance around 400 nm was observed for H9A, H10A, and H9A/H10A (Fig. 5c). This result suggests that the binding site of heme in these mutants qualitatively differ from the heme-binding site in WT HRG-3. To compare the affinity of the heme to these mutants, we performed absorption titration experiments. Figure 5d shows the change in the absorption at 400 nm for various mutants as a function of heme binding. The best fit was obtained with $x = 0.5$ (see the data analysis), where one heme molecule is bound to two HRG-3 monomers, thus confirming the dimer nature of HRG-3. Interestingly, the binding affinity of heme to HRG-3 (H9A) is better than to WT HRG-3, $K_d = 150 \pm 40$ μM and $K_d = 220 \pm 60$ μM, respectively, and the binding affinity of heme to HRG-3 (H10A) is much lower than to WT HRG-3, $K_d = 460 \pm 90$ μM. The heme binding to double mutation HRG-3 (H9A/H10A) has similar affinity, $K_d = 230 \pm 60$ μM, to WT HRG-3. The titration experiments confirmed that the binding of heme to HRG-3 is affected by the H9A and H10A mutations without abolishing it.

The comparable low binding affinity of heme to HRG-3, ~ 200 μM [4], may indicate that heme is not directly coordinated to HRG-3, but rather that it is buried in a hydrophobic core in the protein. Alternatively, other residues in the protein may be involved in heme coordination, although this is unlikely since His residues should have a higher affinity to heme molecules than to other residues in HRG-3 [29–31]. Clearly, mutations in HRG-3 influence its conformational state, affect the binding site of heme, and alter its affinity for hemin. Since HRG-3 is postulated to be a heme-ferrying protein or hemochaperone, the lack of direct heme coordination may allow HRG-3 to

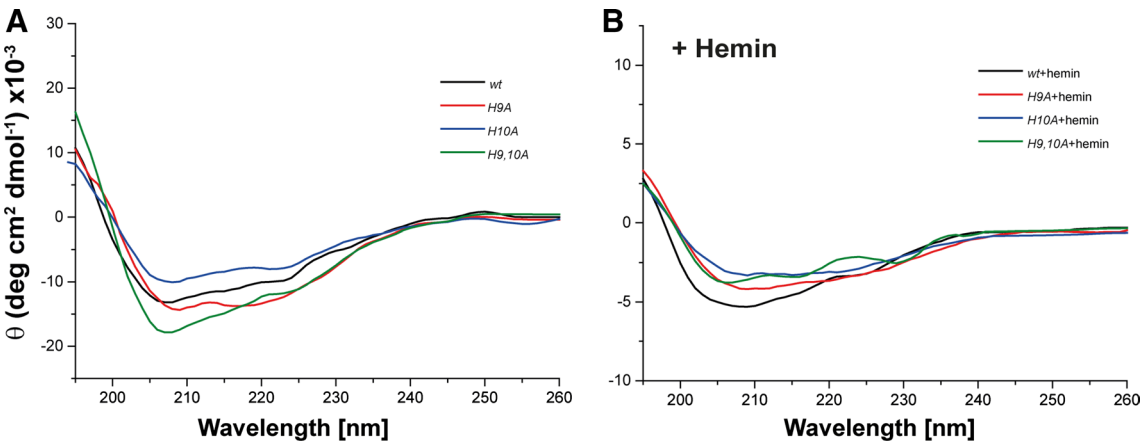

Fig. 6 CD spectra of HRG-3 mutants. **a** In the absence of hemin and **b** in the presence of hemin

Table 2 CD spectral analysis of HRG-3 mutants

	%	+Hemin (%)
WT HRG-3		
α-helix	12.5	12
β-sheet	50	48
Random coil	37.5	40
HRG-3 (H9A)		
α-helix	12.5	10
β-sheet	50.5	48
Random coil	37	42
HRG-3 (H10A)		
α-helix	12	10
β-sheet	51	48
Random coil	37	42
HRG-3 (H9A/H10A)		
α-helix	13	10
β-sheet	50	48
Random coil	37	42

more readily exchange or deliver heme with its target. It is plausible that ancillary proteins may be present to either enhance heme binding to HRG-3 and/or direct HRG-3 targeting to the embryo in vivo. Given that *C. elegans* lack all eight genes for heme biosynthesis, heme synthesis intermediates, including porphyrins, should not normally exist in the worm precluding them as likely ligands for HRG-3 in the secretory pathway. Since worms do need B12 to grow, there is the possibility that HRG-3 may bind this tetrapyrrole. However, the embryonic lethality associated with *hrg-3* mutant worms can only be rescued by heme supplementation and not by B12 or other porphyrins [8].

Our results also indicate that HRG-3 is highly dynamic and flexible, as observed by the RT CW EPR spectra, and therefore, it adopts variations in its sequence and structure; this feature may allow heme binding in HRG-3 mutants, albeit at lower binding affinities. The dynamic nature of metallochaperones has also been reported before for human copper metallochaperone, Atox1 [32].

To further explore the changes in the secondary structure of the protein upon heme binding, CD measurements were performed. CD spectra of various HRG-3 mutants are presented in Fig. 6, and CD spectral analysis by CDNN software is shown in Table 2 [33]. The CD spectra and analysis show that in the presence and absence of hemin all mutants have a similar secondary structure, wherein about 48–50 % of the protein contains beta sheet and 37–42 % random coils. Usually, it is expected that upon ligand binding, a protein adopts more ordered conformations [34]. The fact that we did not observe this supports our proposal that the heme molecule is not directly coordinated to HRG-3 but is buried within a hydrophobic core.

Conclusions

In this study, our aim was to explore one of the few heme chaperones in eukaryotic systems that have been identified to date. HRG-3 mobilizes heme from the intestine to extra-intestinal tissues in *C. elegans*. Mature HRG-3 is a 42 amino acid protein whose hydrophobicity and aggregation limit the biophysical tools that can be used to characterize it. Despite these limitations, EPR spectroscopy and absorption spectroscopy identified some interesting features of HRG-3 structure and heme-binding site. We show that the affinity of heme binding to HRG-3 dimers is about 200 μM. H9 and H10 are significant residues that preserve a specific conformational state of the dimer upon heme binding. Moreover, heme binding occurs closer to the N-terminus of HRG-3 rather than to its C-terminus. H9A and H10A mutants can still bind heme, but with a different

affinity. Our results indicate that HRG-3 is highly dynamic and flexible, and therefore it can adjust to changes that occur in its structure and sequence. Our results support the notion that heme is not directly coordinated to HRG-3, but rather, it is incorporated into a hydrophobic core in the HRG-3 dimer, which may allow it to exchange heme readily with its target. Our study lays the groundwork for future research involving the determination of other key residues that are essential either for heme binding to HRG-3, or for the trafficking of heme from either upstream or downstream interactors of HRG-3.

Acknowledgments This work was supported by funds received from Bar Ilan University.

References

1. Ajioka RS, Phillips JD, Kushner JP (2006) BioChem BioPhys Acta 1763:723–736
2. Schultz IJ, Chen C, Paw BH, Hamza I (2010) J Biol Chem 285:26753–26759
3. Severance S, Hamza I (2009) Chem Rev 109:4596–4616
4. Yuan X, Fleming MD, Hamza I (2013) Curr Opin Chem Biol 17:204–211
5. Yuan X, Prochenko O, Philpott CC, Hamza I (2012) J Biol Chem 287:4914–4924
6. Philpott CC (2012) J Biol Chem 287:13518–13523
7. Chen C, Samuel TK, Krause M, Dailey HA, Hamza I (2012) J Biol Chem 287:9601–9612
8. Chen C, Samuel TK, Sinclair J, Dailey HA, Hamza I (2011) Cell 145:720–731
9. Hamza I (2006) ACS Chem Biol 1:627–629
10. Severance S, Rajagopal A, Rao AU, Cerqueira GC, Miterva M, El-Sayed N, Krause M, Hamza I (2010) PLoS Genet 6:e1001044
11. Rao AU, Carta LK, Lesuisse E, Hamza I (2005) Proc Natl Acad Sci 102:4270–4275
12. Aramini JM, Hamilton K, Rossi P, Ertekin A, Lee H-W, Lemak A, Wang H, Xiao R, Acton TB, Everett JK, Montelione GT (2012) Biochemistry 51:3705–3707
13. Saiki RK, Gelfand DH, Stoffel S, Scharf SJ, Higuchi R, Horn GT, Mullis KB, Erlich HA (1988) Science 239:487–491
14. Peterson GL (1997) Anal Biochem 83:346–356
15. Del Vecchio M, Pogni R, Baratto MC, BNobbs A, Rappuoli R, Pizza M, Balducci E (2009) J Biol Chem 284:33040–33047
16. Peisach J, Blumberg WE, Lode ET, Coon MJ (1971) J Biol Chem 246:5877–5881
17. Hubbell WL, Gross A, Langen R, Lietzow MA (1998) Curr Opin Struct Biol 8:649–656
18. Puljung MC, DeBerg HA, Zagotta WN, Stoll S (2014) Proc Natl Acad Sci 111:9816–9821
19. Joseph B, Morkhov VM, Yulikov M, Jeschke G, Bordignon E (2014) J Biol Chem 289:3176–3185
20. Atherton NM (1993) Principles of electron spin resonance. Ellis Horwood PTR Prentice Hall, England
21. Weil JA, Bolton JR (2007) Electron paramagnetic resonance. Wiley, Hoboken
22. Eaton G, Eaton SS (1989) In biological magnetic resonance. Plenum, New York
23. Freed JH (1976) In spin labeling (theory and applications). Academic Press, New York
24. Gorcester J, Millhauser GL, Freed JH (1990) In modern pulsed and continuous wave electron spin resonance. Wiley, New York
25. McConnell HM (1998) In: Foundations of modern EPR. World Scientific, Singapore
26. Budil DE, Lee S, Saxena S, Freed JH (1996) J Magn Reson Ser A 120:155–189
27. Klare JP (2013) Biol Chem 394:1281–1300
28. Huynh C, Yuan X, Miguel DC, Renberg RL, Protchenko O, Philpott CC, Hamza I, Andrews NW (2012) PLoS Pathog 8:e1002795
29. Yoo B-K, Lamarre I, Martin J-L, Rappaport F, Negrerie M (2015) Proc Natl Acad Sci 112:E1697–E1704
30. Yoo B-K, Lamarre I, Martin J-L, Andrew CR, Negrerie M (2013) J Am Chem Soc 135:3248–3254
31. Vidossich P, Magistrato A (2014) Biomolecules 4:616–645
32. Benitez JJ, Keller AM, Huffman DL, Yatsunyk LA, Rosenzweig AC, Chen P (2011) Faraday Discuss 148:71–82
33. Bohm G, Muhr R, Jaenicke R (1992) Protein Eng 5:191–195
34. Berlow RB, Dyson HJ, Wright PE (2015) FEBS Lett. 589:2433–2440